1 April 1999

OPTICS COMMUNICATIONS

ELSEVIER

Optics Communications 162 (1999) 148–154

Full length article

Transient hole-burning for systems with a noncorrelated frequency exchange

Haiyu Wang *, Shihua Huang

Laboratory of Excited State Processes, and Changchun Institute of Physics, Academia Sinica, Changchun 130021, China

Received 22 July 1998; received in revised form 1 December 1998; accepted 1 December 1998

Abstract

The exact solution of the transient hole-burning (THB) shape has been obtained for systems with a noncorrelated spectral exchange. The THB shapes have been studied for various values of pump Rabi frequency $\chi/2\pi$, time duration and pump–probe time separation. It is shown that the correlated line is dominant in the slow spectral diffusion limit, and it decays with $1/e$ time of the correlation time τ_c; in the fast limit, the hole is mainly determined by the width of the equilibrium frequency distribution a. When $\chi \to 0$, the linewidths are $\sim 3/\pi\tau_c$ and $2a/\pi$ in the slow and fast limit, respectively. The model fails to explain the THB experiments in ruby. However, it is more suitable to describe the FID behaviors under the same experimental condition [V.S. Malinovsky, A. Szabo, Phys. Rev. A 55 (1997) 3826]. © 1999 Elsevier Science B.V. All rights reserved.

PACS: 42.50.Md
Keywords: Transient hole-burning; Random frequency modulation; Optical dephasing

1. Introduction

Coherent transient phenomena provide sensitive techniques to investigate the dynamical processes in low temperature impurity-ion crystals leading to optical dephasing. It is well known that the optical Bloch equations (OBE) are commonly used to describe these processes. However, in magnetic systems, experiments have shown serious discrepancies with the predictions of OBE [1–4]. In these systems, the optical transition frequency has random fluctuations induced by the spin flip-flops of the impurity ions or nuclei in the host lattice, which are not considered in OBE. Using the different stochastic models, several studies have been reported to explain the experiments. Two popular theories are based on Gauss–Markov [5,6] and random telegraph [7–10] dephasing models, both simulation [11,12] and theoretical [13] studies have proved that the latter model is more suitable for a paramagnetic ion system at high magnetic field. At low field, the simple modified OBEs for both models were often used, but the agreement with experiments can be gained only for the parameters out of the limit condition required by modified OBEs [2,6]. So the stochastic dephasing models are still not clear.

Recently, Malinovsky and Szabo [14] have studied the free induction decay (FID) behaviors after pulse saturation in systems with a noncorrelated spectral exchange, and demonstrated that the field dependence of FID rates in two experiments had a self-consistent explanation in the limit of the slow spectral diffusion. To further test this model, our study focuses on another coherent phenomenon, transient hole-burning (THB) by the same model. The THB shapes are calculated under the condition of Ref. [3] in both slow and fast spectral diffusion limits, and are compared with the experiments.

* Corresponding author. E-mail: lesp@public.cc.jl.cn

PII: S0030-4018(98)00657-9

2. Transient hole-burning shape

Let us consider an ensemble of impurity ions driven by the radiation field. Each ion is a two-level system (TLS) whose optical transition frequency ω_0 is modulated by $\varepsilon(t)$ caused by a perturbing reservoir. We take the same model of random modulation $\varepsilon(t)$ which was described in Ref. [14], $\varepsilon(t)$ has a Lorentzian equilibrium distribution $\varphi(\varepsilon)=(1/\pi)[a/(\varepsilon^2+a^2)]$, and it changes instantly then remains constant until the next jump; the jump rate is $1/\tau_c$. A pump pulse $E_1\exp[i\omega_1 t]$ within time T interacts with the system to burn a hole, and after time t_d, a weak probe pulse $E_2\exp[i\omega_2 t]$ is used to monitor the hole shape. In general, the observed hole shape at time τ can be expressed as [15]:

$$n(\Delta,\chi,\tau)=\mathrm{Re}\int_{T+t_d}^{\tau}\mathrm{d}t\int\mathrm{d}\omega\overline{n(\omega,T,\tau-t)}$$

and

$$\overline{n(\omega,T,\tau-t)}=\left\langle n(\omega,\varepsilon,T)\exp\left\{i(\omega-\Delta-i/T_2)(\tau-t)+i\int_t^{\tau}\varepsilon(t')\mathrm{d}t'\right\}\right\rangle \tag{1}$$

Here $\omega=\omega_0-\omega_1$ is the pump detuning, $\Delta=\omega_2-\omega_1$, $\chi/2\pi$ is the pump Rabi frequency, $n(\omega,\varepsilon,T)$ is the stochastic population difference at the end of the pump pulse, $\langle\dots\rangle$ denotes averaging over the random process $\varepsilon(t)$, the integration over ω results from the inhomogeneous distribution caused by the crystal field dispersion, and T_1 is the spontaneous lifetime of the upper state ($T_2=2T_1$).

The hole spectrum contains the average of the product of two functions, $n(\omega,\varepsilon,T)$ and $\exp[i\int_t^{\tau}\varepsilon(t')\mathrm{d}t']$, which depend on the values of the random fluctuation during pump and probe time intervals, $[0,T]$ and $[t,\tau]$. If the time separation t_d is much larger than the correlation time τ_c, the average in Eq. (1) can be factored into the product of $\langle n(\omega,\varepsilon,T)\rangle$ and of the relaxation function $K(\tau-t)=\langle\exp[i\int_t^{\tau}\varepsilon(t')\mathrm{d}t']\rangle$. When $t_d\to 0$ and the probe pulse is short, the stochastic processes in the two time intervals are completely correlated just like FID, and the stochastic averaging in Eq. (1) can be described as [14,16]:

$$\overline{n(\omega,T,\tau-t)}=\exp[i(\omega-\Delta+i/T_2)(\tau-t)]\int n(\omega,\varepsilon,T)K(\varepsilon,\tau-t)\mathrm{d}\varepsilon \tag{2}$$

where $K(\varepsilon,\tau-t)$ is the marginal average.

By a Laplace transformation to Eq. (2), we get:

$$\overline{n(\omega,p,p_1)}=\exp[-i\Delta(\tau-t)]\int n(\omega,\varepsilon,p)K(\varepsilon,p_1)\mathrm{d}\varepsilon \tag{3}$$

where $K(\varepsilon,p_1)=\int_0^{\infty}K(\varepsilon,\tau-t)\exp\{(-p_1+i\omega-1/T_2)(\tau-t)\}\mathrm{d}t$, and one can find the expression in Ref. [14].

To obtain $n(\omega,\varepsilon,p)$, we start from the kinetic equation of the noncorrelated sudden modulation theory [14]:

$$\dot{r}(\varepsilon)=-\hat{L}(\varepsilon)r(\varepsilon)+\varphi(\varepsilon)(\hat{\Gamma}\bar{r}+\hat{\Lambda}) \tag{4}$$

where

$$r(\varepsilon)=\begin{pmatrix}\sigma_{12}(\varepsilon)\\ \sigma_{21}(\varepsilon)\\ n(\varepsilon)\end{pmatrix},\quad \hat{L}(\varepsilon)=\hat{L}_0+i\varepsilon\hat{L}_1+\hat{\Gamma}$$

$$\hat{L}_0 = \begin{pmatrix} \frac{1}{T_2} - i\omega & 0 & -\frac{i\chi}{2} \\ 0 & \frac{1}{T_2} + i\omega & \frac{i\chi}{2} \\ i\chi & i\chi & \frac{1}{T_1} \end{pmatrix}, \quad \hat{L}_1 = \begin{pmatrix} -1 & 0 & 0 \\ 0 & 1 & 0 \\ 0 & 0 & 0 \end{pmatrix}, \quad \hat{\Gamma} = \frac{1}{\tau_c}\hat{I}, \quad \hat{\Lambda} = \begin{pmatrix} 0 \\ 0 \\ \frac{n_0}{T_1} \end{pmatrix}$$

$\sigma_{12} = \sigma_{21}^* = \rho_{12}\ \exp(i\omega t)$, $n = \rho_{22} - \rho_{11}$ is the population difference, n_0 is the equilibrium population difference. The following expressions can be made dimensionless by using a time unit τ_c.

By applying a Laplace transformation to Eq. (4), one can easily obtain the solution of $r(\varepsilon,p)$:

$$r(\varepsilon,p) = \frac{\varphi(\varepsilon)}{p + \hat{L}(\varepsilon)} \hat{\Gamma} \frac{1}{1 - \overline{\varphi(\varepsilon)\hat{\Gamma}/(p + \hat{L}(\varepsilon))}} \hat{\Gamma}^{-1}\left(r_0 + \frac{1}{p}\hat{\Lambda}\right). \tag{5}$$

Then $n(\omega,\varepsilon,p)$ can be expressed as:

$$n(\omega,\varepsilon,p) = \frac{n_0\varphi(\varepsilon)\left[\omega^2 + (a+\kappa)^2\right]}{p(\omega^2 + F^2)} \left\{ 1 + \left(I_1^2 + \kappa^2 I_0^2\right) - \frac{I_0\kappa^2}{p + t_2} - I_0(p + t_2) - \frac{\chi^2\left[p + t_2 - I_0\kappa^2 - I_0(\omega+\varepsilon)\right]}{(p + t_1)\left[(\omega+\varepsilon)^2 + \kappa^2\right]} \right\} \tag{6}$$

where

$$I_0 = \int \frac{\varphi(\varepsilon)\mathrm{d}\varepsilon}{\kappa^2 + (\omega+\varepsilon)^2}, \quad I_1 = \int \frac{\varphi(\varepsilon)(\omega+\varepsilon)\mathrm{d}\varepsilon}{\kappa^2 + (\omega+\varepsilon)^2}, \quad \kappa^2 = (p + t_2)^2 + \frac{p + t_2}{p + t_1}\chi^2,$$

$$F^2 = \left[p + \frac{1}{T_2} + \frac{(p + t_2)a}{\kappa}\right]\left[p + \frac{1}{T_2} + \frac{a\kappa}{p + t_2} + \frac{\chi 2}{p + 1/T_1}\right], \quad t_{1,2} = \frac{1}{T_{1,2}} + 1.$$

By replacing this result into Eq. (3), one can easily get $\overline{n(\omega,p_1,p)}$. After performing the inverse Laplace transformation of $\overline{n(\omega,p_1,p)}$ and integrating with respect to ω in accordance with the general Eq. (1), we can get:

$$\int \overline{n(\omega,T,\tau - t)}\mathrm{d}\omega = \frac{\pi\chi^2 \exp\left[i\Delta(\tau - t)\right]}{pF}\left\{(A - C)\exp\left[-B_1(\tau - t)\right] + C(a + F - \kappa)\exp\left[-B_2(\tau - t)\right]\right\}$$

where

$$A = \frac{p + 1/T_2}{p + 1/T_1} + \frac{(p + t_2)a}{(p + 1/T_1)\kappa}, \quad B_1 = a + F + 1/T_2, \quad B_2 = \kappa + t_2,$$

$$C = \frac{a\{p + 1/T_2 + (p + t_2)(a + F)/\kappa\}}{(a + F - 1 - \kappa)(p + t_1)}. \tag{7}$$

Up to now, the result is obtained under the assumption of complete correlation of the system motion during pump and probe. In another limit case ($t_d \gg \tau_c$), as mentioned above, the stochastic average can be uncoupled, and one can easily get it by directly averaging Eq. (6). The solution can be readily given by Eq. (7) in the limit $C = 0$. Since the correlation of random frequency usually has the form $\exp(-\tau/\tau_c)$, in the more general case, one just needs to substitute C with $C\ \exp[-(\tau - t + t_d)/\tau_c]$ into Eq. (7). This is very similar to the situation when one compares the two-pulse photon echo decay with the three-pulse decay, where the waiting time T_w corresponds to t_d. After integrating with respect to t, we get the final observed hole shape as:

$$n(\Delta,\chi,\tau) = \frac{\pi\chi^2}{pF}\left\{\frac{D_1 A}{\Delta^2 + H_1^2} - \frac{D_2 C^*}{\Delta^2 + H_2^2} + \frac{D_3 C^*(a + F - \kappa)}{\Delta^2 + H_3^2}\right\} \tag{8}$$

where

$$H_1 = B_1,\quad H_2 = B_1 + 1,\quad H_3 = B_2 + 1,\quad C^* = C\exp(-t_d),\quad \theta = \tau - T - t_d$$

$$D_{1,2,3} = H_{1,2,3}\left[1 - \exp(-H_{1,2,3}\theta)\cos\Delta\theta\right] + \Delta\exp(-H_{1,2,3}\theta)\sin\Delta\theta.$$

The factors D_1, D_2 and D_3 are caused by finite probe pulse duration, and usually are not important. In general, the spectral hole is composed of three Lorentzian lines, the second and third lines in Eq. (8) result from the correlation between

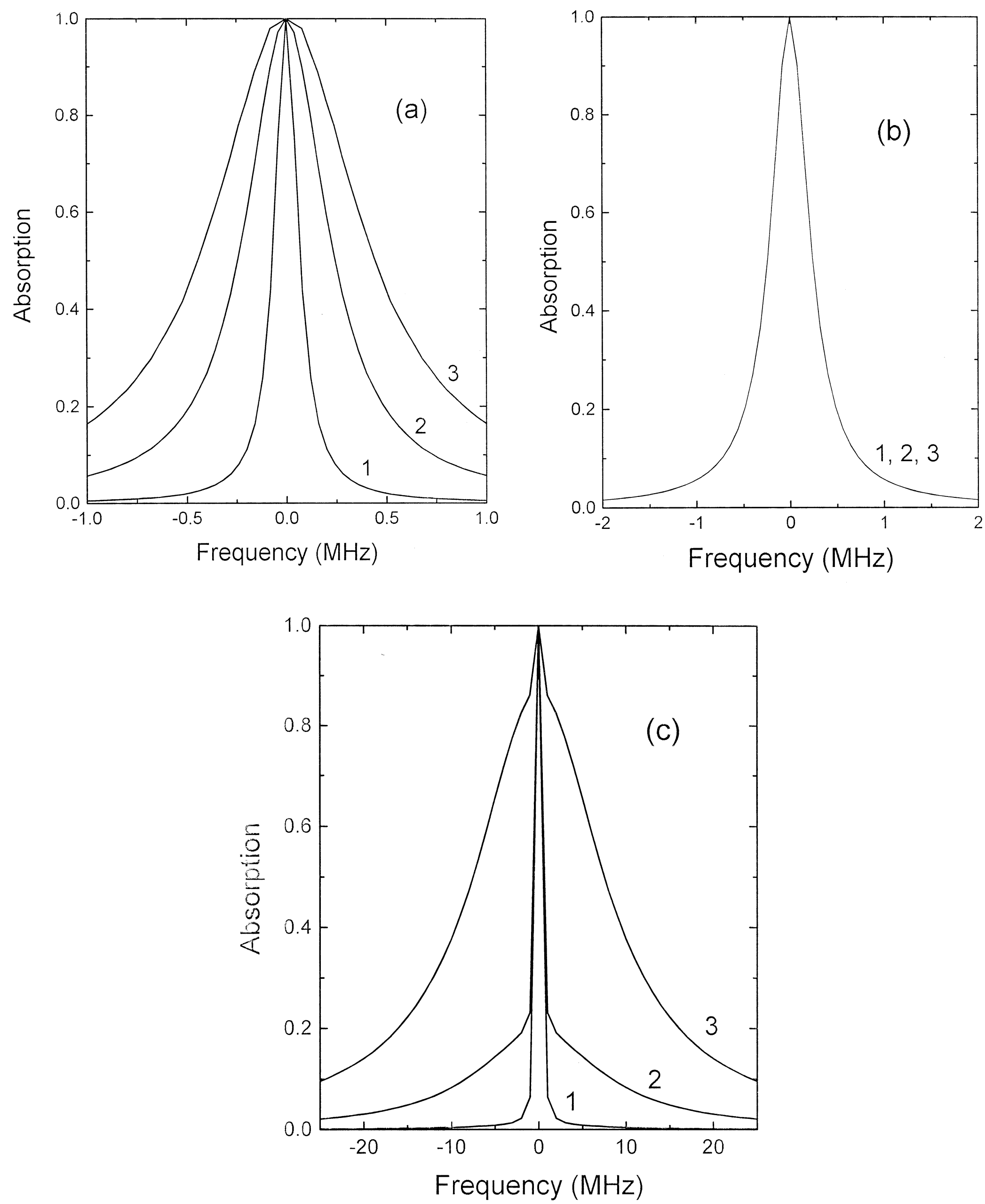

Fig. 1. The hole shapes versus Rabi frequency $\chi/2\pi$, burning time T and pump–probe time separation t_d, $\tau = 2T + t_d$. (a) $T = 50$ μs, $t_d = 10$ μs. The curves 1–3 correspond to $\chi/2\pi = 10$, 100, 200 kHz. (b) $\chi/2\pi = 100$ kHz, $t_d = 10$ μs. The curves 1–3 correspond to $T = 50$, 100, 200 μs. (c) $\chi/2\pi = 100$ kHz, $T = 50$ μs. The curves 1–3 correspond to $t_d = 50$, 100, 150 μs.

the pump and probe duration. Comparing to Eq. (7), the additional linewidth $1/\tau_c$ of these two lines is caused by the correlation decay during the probe pulse. In the limit of complete correlation, as one can expect, the hole reduces to two Lorentzian line-shapes, corresponding to the two exponential decay parts of the FID result [14]. If one neglects the correlation of the system motion during the pump and probe, then C^* in Eq. (8) is zero, the hole is a single Lorentzian line with width $(a+F)/\pi$.

3. Discussion

To explain the experiments, we take the values of parameters a, τ_c on the basis of the photon echo (PE) result. Since the observed echo decay is exponential, we can restrict the discussion to the limit of the slow and fast spectral exchanges, in which the PE decay rates are $1/T_2 + 1/\tau_c$ and $1/T_2 + a$, respectively.

First we consider the slow exchange case, taking $a\tau_c = 200$, $\tau_c = 15$ μs and $T_1 = 4200$ μs, as in Ref. [14]. Fig. 1 shows the normalized hole shape calculated for different values of the Rabi frequency $\chi/2\pi$, burning time T and pump–probe time separation t_d. The hole shapes are expected to contain a broad (H_1) and a narrow (H_3) line (because $1/\pi\tau_c$ contributes only an additional linewidth of 21.2 kHz, the first and second lines in Eq. (8) overlap). But, as we can see in Fig. 1, the hole is a single Lorentzian line, and the linewidth remains unchanged with an increase of the burning time T. The broad line does not appear until $t_d > 100$ μs ($\gg \tau_c$) because the magnitude of the broad line is much smaller than that of the narrow one. So, to obtain a correct hole shape, one cannot neglect the correlation of the system motion, even when $t_d \gg \tau_c$. In Ref. [3], the observed hole contains two lines, and the broad hole became deeper with the increase of χ; when $\chi/2\pi > 100$ kHz and $t_d = 10$ μs, the narrow hole could hardly be separated from the broad one. That is to say, the broad line H_1 does not correspond to the observed one. In addition, the hole shapes do not exhibit any nutation structure that was predicted by the conventional and modified OBEs [3,6].

For the fast diffusion limit case, we take $a/2\pi = 10.6$ kHz, $a\tau_c = 1/15$. As mentioned in Ref. [16], the solution agrees well with the perturbation theory, and one can neglect the correlation between the pump and probe duration. Fig. 2 shows the hole shapes that are calculated by applying the condition of Ref. [3], $T = 50$ μs, $t_d = 10$ μs and $\tau = 110$ μs. We can see that only one line (H_1) appears. Since the shapes contain single Lorentzian lines for both slow and fast spectral diffusion cases, we try to explain the narrow hole behaviors in Ref. [3] in these two limits. To compare with the experimental results, we take into account the Gaussian shape of the laser beam used in the experiments; the calculated half-width varies with χ as shown in Fig. 3. One can find that the results are not satisfied in both limits. As in other theories [2,6,16,17], it seems that

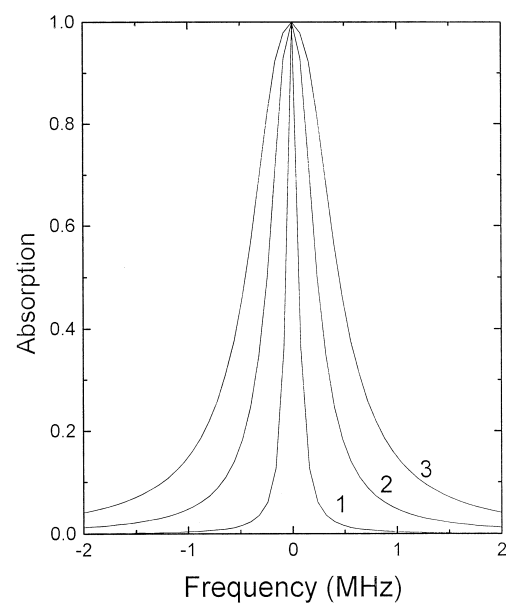

Fig. 2. The hole shapes versus Rabi frequency $\chi/2\pi$ in the fast spectral diffusion limit. The curves 1–3 correspond to $\chi/2\pi = 10$, 50, 100 kHz.

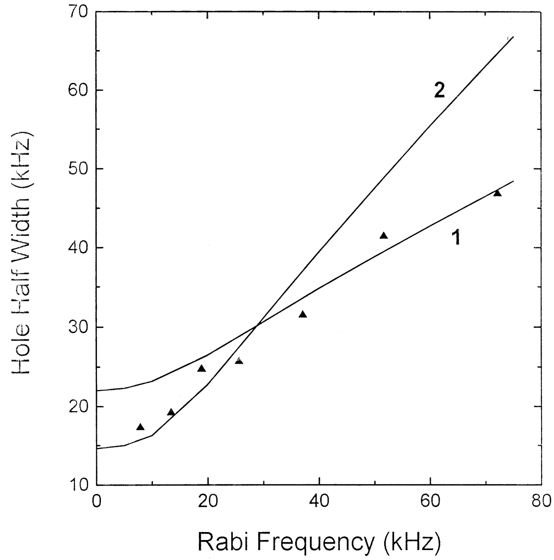

Fig. 3. Field dependence of the hole half-width for a Gaussian shaped beam. The solid curve 1, calculated in slow spectral diffusion limit; 2, in the fast limit; ▲, experimental data [3].

the parameters of best fitting to the experiments are also outside the fast or slow diffusion limit, for which PE is non-exponential.

In the slow limit, the discrepancy is obviously due to the additional linewidth. When $\chi \to 0$, using Eq. (8), one can get the hole shape to second-order in χ:

$$n(\Delta,\tau) = \frac{\pi\chi^2}{p}\left\{\frac{1}{p+1/T_1}\,\frac{p+2(a+1/T_2)}{\Delta^2+4(p/2+a+1/T_2)^2}\right.$$
$$\left.+\exp\left(-\frac{t_d}{\tau_c}\right)\frac{a\tau_c(2a\tau_c-1)}{2(p+t_1)(a\tau_c-1)}\,\frac{p+2(3/2\tau_c+1/T_2)}{\Delta^2+4(p/2+3/2\tau_c+1/T_2)^2}\right\}. \quad (9)$$

Here, we have neglected the unimportant line H_2. At the center of the lines, the magnitude of the second line H_3 is about hundred times larger than that of the first line H_1. So line H_3 dominates in the slow limit, and the value of the width of the hole ($\sim 3/\pi\tau_c$) differs from that of the decay rate of FID ($\sim 2/\pi\tau_c$) when $\chi \to 0$. However, they are the same in the fast diffusion limit, $\sim 2a/\pi$.

In spite of these discrepancies, there are still some questions. In fact, the dephasing mechanism in ruby is much more complex. At low magnetic field, there are two main sources of the spectral exchange. One is controlled by Cr–Cr electron spin interaction, the estimated width of static magnetic broadening is about 70 kHz [3]; another is due to the superhyperfine interaction of Cr–Al, the width is about 1.2 MHz [18], but the major contribution of broadening results from Al nuclei in the frozen core, the flip rate of Al spins is only about 1/1200 μs [19]. So, one can hardly find an interaction (τ_c is close to 15 μs) in ruby which contributes to the large static broadening $a/\pi = 4.2$ MHz used in the slow spectral diffusion limit. This problem also occurred when one tried to explain FID behaviors in LaF_3:Pr^{3+} by the same model [16]. In addition, the observed narrow hole collapsed into the broad line with 1/e time of 300 μs [3], as a result of the spectral diffusion caused by the superhyperfine interaction of Cr–Al, not the decay of the narrow hole itself. But, under this model, the narrow line H_3 decays with a 1/e time of τ_c, it is contradicting the observation. In the fast limit, the power broadening notably increases with the increase of burning time, in contrast with the fact that the linewidth of the observed narrow hole almost remained unchanged [3].

In summary, the noncorrelated frequency exchange model fails to explain the THB experiments in ruby for both slow and fast diffusion limit cases. However, it is more appropriate to describe the FID behaviors under the same experimental condition [14].

Finally, it is interesting to compare the hole behavior in the fast diffusion limit with that of the conventional OBE. Under the condition of cw pump, the hole shape can be obtained in the limit $\lim_{p\to 0} pn(\Delta,\chi,\tau)$, and the linewidth H_{cw} is given by:

$$H_{cw} = a\left\{1 + \sqrt{1 + \frac{T_1\chi^2}{a\sqrt{1+\chi^2\tau_c^2}}}\right\} \tag{10}$$

where we neglect the very small terms $1/T_1$ and $1/T_2$. Remembering that $1/a$ corresponds to the transversal relaxation time T_2 in the conventional OBE, and τ_c often has a small value, thus H_{cw} is the same as the conventional OBE result in the fast diffusion limit.

4. Conclusion

The exact solution of the THB shape under noncorrelated spectral exchange has been obtained. In general, the hole contains three Lorentzian lines, two of them arise from considering the correlation of the system motion during pump and probe time intervals.

The THB shape has been calculated for different values of χ, T and t_d. It is shown that the holes contain only the correlation line H_3 in the slow spectral diffusion limit, and decay with 1/e time of τ_c; in the fast limit, the solution approximately coincides with the result of the perturbation theory, and only the noncorrelation line H_1 appears. For both limit cases, the model fails to explain the narrow hole behaviors in Ref. [3], however, the FID behaviors have been explained successfully by this model [14]. This disagreement may be related to different diffusion mechanisms operating over different time scales for THB (> 100 μs) and FID (~ 10 μs) experiments.

When $\chi \to 0$, the linewidths are equal to $(2/T_2 + 3/\tau_c)/\pi$ and $2(1/T_2 + a)/\pi$ in the slow and fast limit, respectively. This coincides with PE and FID rates in the fast limit, while it is different in the slow one.

Acknowledgements

The authors are grateful for the financial support of the National Natural Science Foundation of China.

References

[1] R.G. Devoe, R.G. Brewer, Phys. Rev. Lett. 50 (1983) 1269.
[2] A. Szabo, T. Muramoto, Phys. Rev. A 39 (1989) 3992.
[3] A. Szabo, R. Kaarli, Phys. Rev. B 44 (1991) 12307.
[4] J. Ganem, Y.P. Wang, D. Boye, R.S. Meltzer, W.M. Yen, Phys. Rev. Lett. 66 (1991) 695.
[5] E. Hanamura, J. Phys. Soc. Jpn. 52 (1983) 2258.
[6] A. Szabo, T. Muramoto, Phys. Rev. A 37 (1988) 4040.
[7] K. Wodkiewicz, J.H. Eberly, Phys. Rev. A 32 (1985) 992.
[8] P.R. Berman, R.G. Brewer, Phys. Rev. A 32 (1985) 2784.
[9] V.S. Malinovsky, Phys. Rev. A 52 (1995) 4921.
[10] H. Wang, H. Li, S. Huang, Phys. Rev. A 54 (1996) 3381.
[11] R.S. Meltzer, J. Ganem, Y.P. Wang, D. Boye, W.M. Yen, D.P. Landau, Wannemacher, R.M. Macfarlane, J. Lumin. 53 (1992) 1.
[12] S. Huang, A. Szabo, J. Lumin. 68 (1996) 291.
[13] H. Wang, S. Huang, Physica B 239 (1997) 261.
[14] V.S. Malinovsky, A. Szabo, Phys. Rev. A 55 (1997) 3826.
[15] A.P. Nizovtsev, N.S. Onishchenko, Opt. Spectrosc. 74 (1993) 573.
[16] A.I. Burshtein, A.A. Zharikov, V.S. Malinovsky, Phys. Rev. A 43 (1991) 1538.
[17] S.Ya. Kilin, A.P. Nizovtsev, J. Lumin. 64 (1995) 69.
[18] T. Endo, T. Muramoto, T. Hashi, Phys. Lett. A 99 (1983) 128.
[19] A. Szabo, T. Muramoto, R. Kaarli, Phys. Rev. B 42 (1990) 7769.